We are IntechOpen,
the world's leading publisher of
Open Access books
Built by scientists, for scientists

4,800
Open access books available

122,000
International authors and editors

135M
Downloads

154
Countries delivered to

Our authors are among the

TOP 1%
most cited scientists

12.2%
Contributors from top 500 universities

CLARIVATE ANALYTICS
BOOK CITATION INDEX
INDEXED

WEB OF SCIENCE™

Selection of our books indexed in the Book Citation Index
in Web of Science™ Core Collection (BKCI)

Interested in publishing with us?
Contact book.department@intechopen.com

Water as a Refrigerant in Centrifugal Compressor Cooling Systems for Industrial Applications

Florian Hanslik and Juergen Suess

Abstract

As a consequence of the F-gas regulation R404A is no longer a viable option for commercial refrigeration applications. Therefore, this paper focuses on natural refrigerants. There are a few alternatives like carbon dioxide, which has an efficiency loss with increasing environment temperatures. A promising option is the combination of a carbon dioxide process with a chiller using water as refrigerant. Two types of interconnection seem to make energy sense. On the one hand, the interconnection as a cascade, whereby the complete heat of condensation is given off to the water chiller, on the other hand the subcooling of transcritical CO_2 after the gas cooler. Both types of interconnection result in optimized operating parameters for the CO_2 process. These are examined more closely, and finally, the annual COP values are compared with the standard systems.

Keywords: refrigeration, water, carbon dioxide cascade, subcooling, vapor compression, chiller, energy efficiency

1. Introduction

The F-gas regulation, which came into force on January 1, 2015, envisages an EU-wide phase-down of the CO_2 equivalent of hydrofluorocarbons (HFCs) by 79% by 2030 compared to a reference value based on the annual average of the quantities of hydrofluorocarbons, a producer or importer reported to have placed in the market between 2009 and 2012. From January 1, 2020, the next step will be a ban of placing refrigeration appliances for commercial use with HFCs with GWP > 2500 [1]. As a result, the refrigerant blend R404A may no longer be used in new systems from this point in time.

A current alternative is HFC or HFO replacement, but in most cases, they are only seen as a temporary solution. A long-term alternative is natural refrigerant. Water stands out as a natural refrigerant because it has no GWP or ODP and is neither flammable nor toxic. When used in a refrigeration system, it occurs in the liquid and gaseous states. The thermodynamic process takes place in a rough vacuum due to the vapor pressure curve of water but then corresponds to the cycle of conventional refrigeration systems.

In this chapter, the properties of water as a refrigerant are considered in more detail, an overview of previously implemented systems is given, and the mode of operation and special features of such a system are explained. Using examples, the promising field of applications gets defined, and the efficiency of the systems is shown.

2. Water as refrigerant

2.1. The thermodynamic properties of water

Water (R718) as a refrigerant is one of the oldest fluids being used for refrigeration applications down to about the freezing point. When water is coupled with protective solutions to prevent freezing (i.e., propylene or ethylene glycol), it can also be used well below water's normal freezing point in applications such as ice slurries. Water is easily available and has excellent thermodynamics and chemical properties. It was found by reference [2] that for evaporator temperatures above 20°C R718 gives the highest COP of all refrigerants assuming exactly the same cycle parameters [3].

Figure 1 shows the vapor pressure curves of various refrigerants. In the case of R718, it is noticeable that the pressures in the temperature range for a typical cooling application in server rooms are between 10 and 100 mbar.
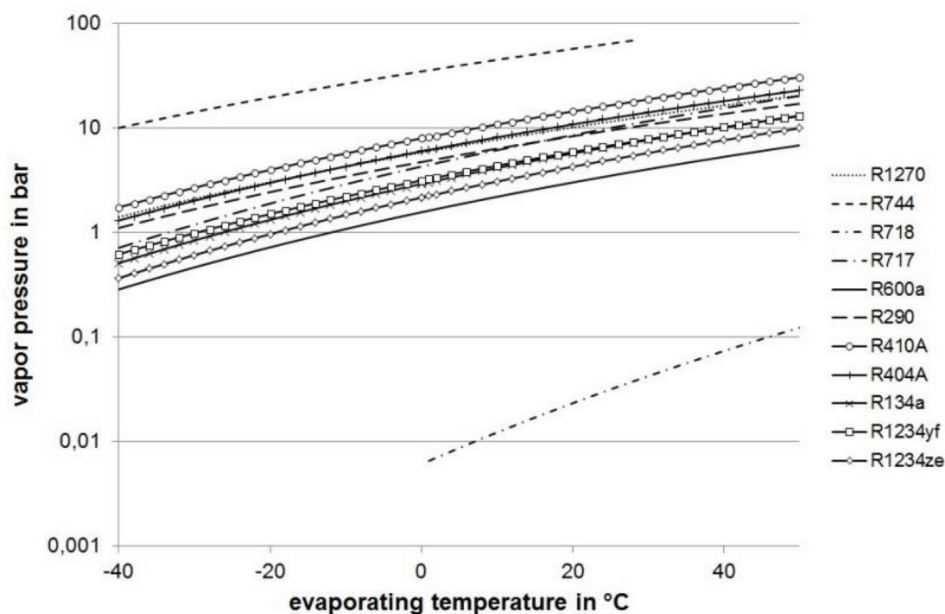

Figure 1. Vapor pressure curves of selected refrigerants.

In addition to the necessary operation in a rough vacuum, **Figures 2** and **3** show the low volumetric cooling capacity and the high required pressure ratio of water as a refrigerant compared to conventional refrigerants.

Both properties require an optimal compressor concept as well as optimum flow control of the water vapor, as this is the only way to minimize the possible losses and to use the advantages of water as a refrigerant efficiently.

The curves of the respective refrigerants in **Figures 1–3** were calculated using REFPROP [4].

2.2. Compressor cooling systems for the refrigerant water

Up to now, quite a few centrifugal chillers were built with R718 as working fluid. In **Table 1** the most relevant projects are listed. The cooling capacity of the majority of the machines is typically above 500 kW, and all machines use centrifugal compressors with the exception of the chiller described by reference [5]. Here, a positive displacement compressor of the Roots blower type is applied. The centrifugal compressors are either of the axial type with up to seven stages or use radial impeller designs with typically two stages. In most machines inter-cooling between the stages is realized, as water vapor has a rather high discharge temperature due to its large polytropic index of approximately 1.33 in the operational range of the compressor [3].

While R718 as refrigerant is state of the art in absorption chillers with lithium bromide as absorbent, none of the mechanical water vapor compression machines shown in **Table 1** have reached a commercially viable status so far, and their market penetration is still pending. According to Ophir [6], only IDE Technologies which is an Israelian water desalination company has successfully built and commissioned a significant number of installations in the field, which still cannot be regarded as industrialized mass-produced machines [3].
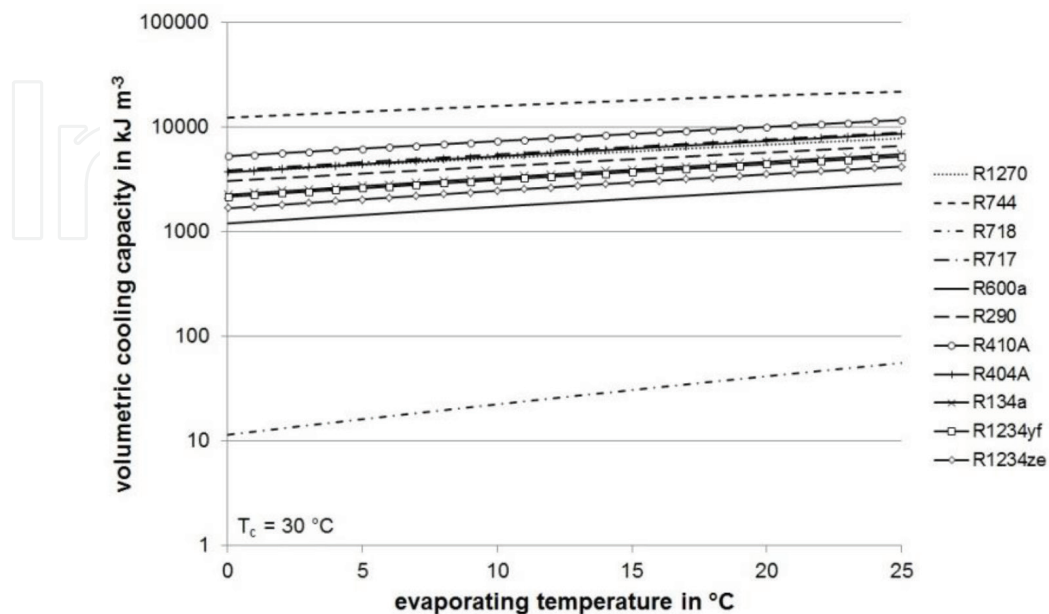

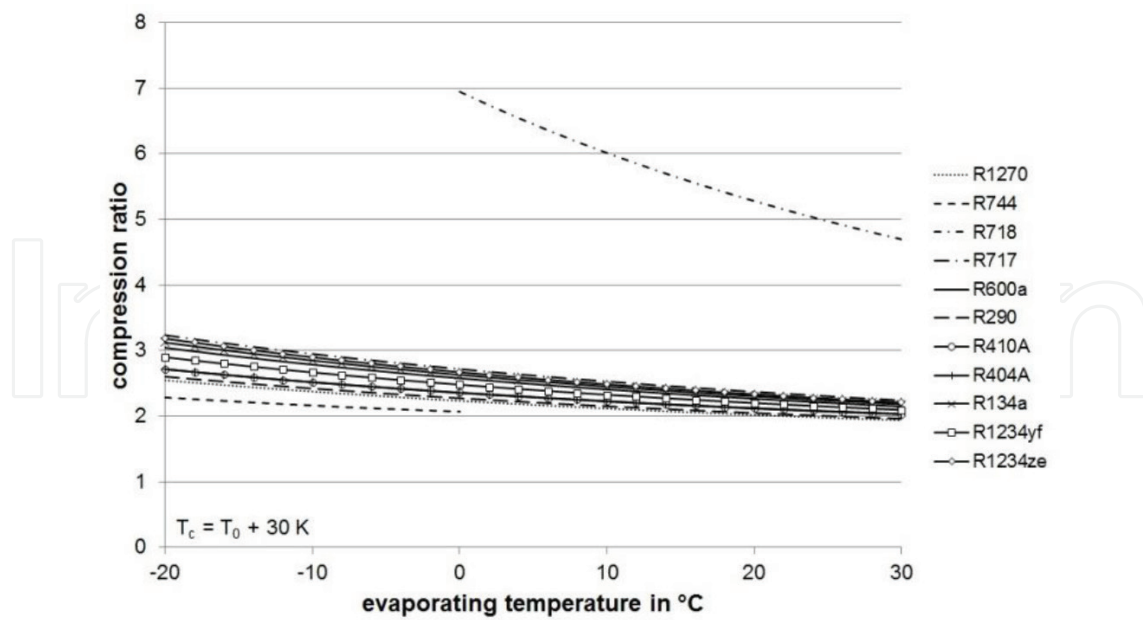**Figure 2.** Volumetric cooling capacities of selected refrigerants.

Figure 3. Required compression ratios of selected refrigerants.

Year	Location	Project group	Application	Cooling capacity	Literature source
1990	Denmark	IDE/Sabroe	Sea water heat pump	1.3 MW	[6]
1995	Denmark	IDE/Sabroe/TI	Plastic molding cooling	2 MW	[6]
1995	RSA	IDE/Integral	Gold mine cooling	6 × 3 MW	[6]
1999	Germany	ILK/GHS Essen	Chilled water	1 MW	[7]
1999	Germany	ILK/VW	Chilled water	1 MW	[8]
2000	Germany	ILK/Daimler	Chilled water	1 MW	[7]
2002	Japan	IDE/Sanken	Vacuum ice	350 kW	[6]
2007	Japan	IDE/Nissan	Vacuum ice	1.5 MW	[6]
2008	RSA	IDE	Gold mine cooling	3 × 3 MW	[6]
2008	Switzerland	IDE	Artificial snow	1.4 MW	[6]
2008	Austria	IDE	Artificial snow	1.4 MW	[6]
2011	USA	MSU	Chilled water	—	[9]
2012	Denmark	Rotrex/Topsøe	Heat pump	350 kW	[10]
2013	Japan	Kawasaki HI	Chilled water	350 kW	[11]
2012	Germany	ILK/Cofely Ref.	Chilled water	800 kW	[12]
2014	Japan	Sasakura	Chilled water	17.5 kW	[5]
2015	Denmark	TI/JCI	Chilled water	800 kW	[13]
2015	Germany	ILK	Vacuum ice	50 kW	[12]
2015	Germany	efficient energy	Chilled water	35 kW	[14]

Table 1. Centrifugal chiller projects using R718 as refrigerant [3].

3. Centrifugal compressor cooling system

The functional and working process of a compact compression refrigeration system with the refrigerant water is explained below.

The chiller fulfills two tasks: on the one hand, the cooling of the chilled water to the desired cold water outlet temperature and, on the other hand, the removal of the heat extracted from the water from a heat source. Of importance are the two identical refrigeration modules, one of which is shown in **Figure 4**. Each refrigeration module comprises the complete thermodynamic cycle. The evaporator and the condenser are nested to achieve a compact design. The chilled water enters the evaporator via the middle connection of the refrigeration module at a flow rate of approx. 2 liters per second. Here, there is a pressure that corresponds to the saturated pressure of the desired water outlet temperature of the evaporator. It is evaporated so much water until the superheated water has cooled to saturation temperature. The chilled cold water is directed downward out of the module. The maximum resulting vapor mass corresponds to about 1% of the circulated mass flow of water. The vapor enters the centrifugal compressor and is compressed to a higher pressure and temperature. The maximum achievable pressure ratio is currently in the range of 3.5 due to the rotational speed limitation of the compressors. The compression starts at approx. 40,000 revolutions per minute with a pressure ratio of 1 and can be continuously increased from there up to the maximum pressure ratio. The compressed, superheated steam flows into the condenser where it meets the cooling water. The cooling water is also fed to the cooling module from below. Due to the special design of the condenser, it is achieved that the water vapor can deliver its complete energy
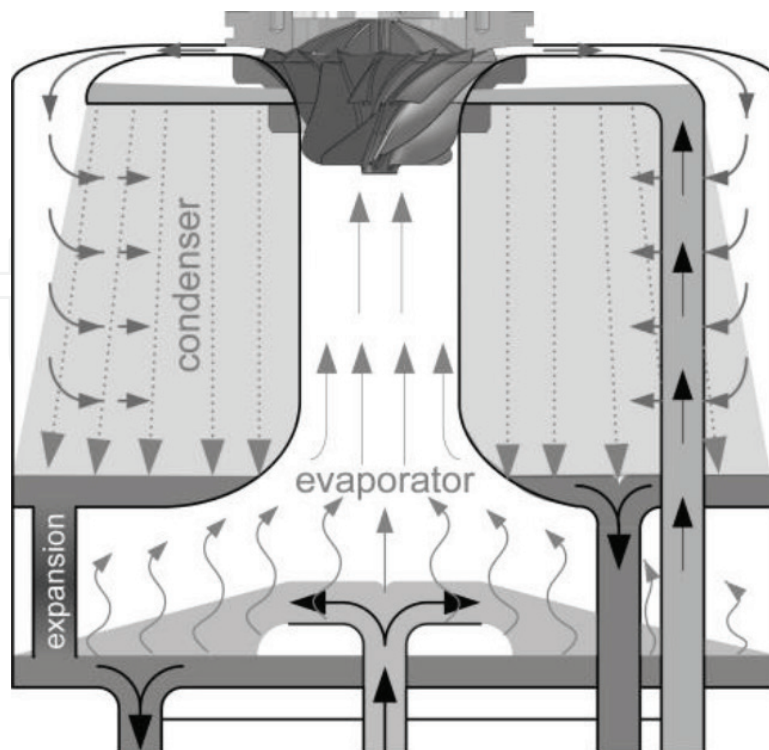

Figure 4. Schematic drawing of the cooling module.

to the circulating cooling water and gets completely condensed. The heated cooling water is discharged down from the module. To close the thermodynamic cycle, the evaporated amount of water from the condenser is returned via the self-regulating expansion device in the evaporator.

Depending on the heat sink temperature, this process can be followed by the second cooling module as a cascade.

4. Combination with water-loop cooled self-contained units

This subsection investigates the combination of a CO_2 process of a self-contained unit with water-loop cooling and a compression refrigeration unit with the refrigerant water in a cascade arrangement.

4.1. Basics

4.1.1. R744 cycle

The basic structure of a single-stage R744 refrigeration cycle is shown in **Figure 5**. Depending on the heat sink temperature, a distinction is made between a subcritical system and a transcritical system. The mode of operation determines the selection of components to a considerable extent.

4.1.2. R718 cycle

The properties of R718 shown in Chapter 2.1 set the following requirements for the use of water as a refrigerant. The low vapor pressures require operation in vacuum, and the large pressure ratio requires a two-stage compression in cascade.

An overview of the machines implemented and the technical challenges of using water as a refrigerant in a centrifugal compressor cooling system have been described by reference [3].

Figure 6 shows a one-step process for both systems (a) and (b). This is for simplification of the illustration only. In the later calculation, however, the real two-stage operation is considered.
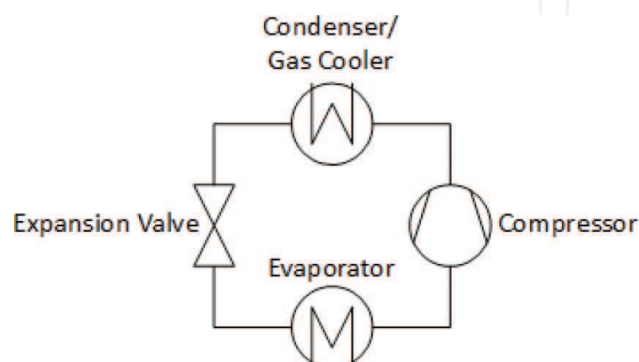

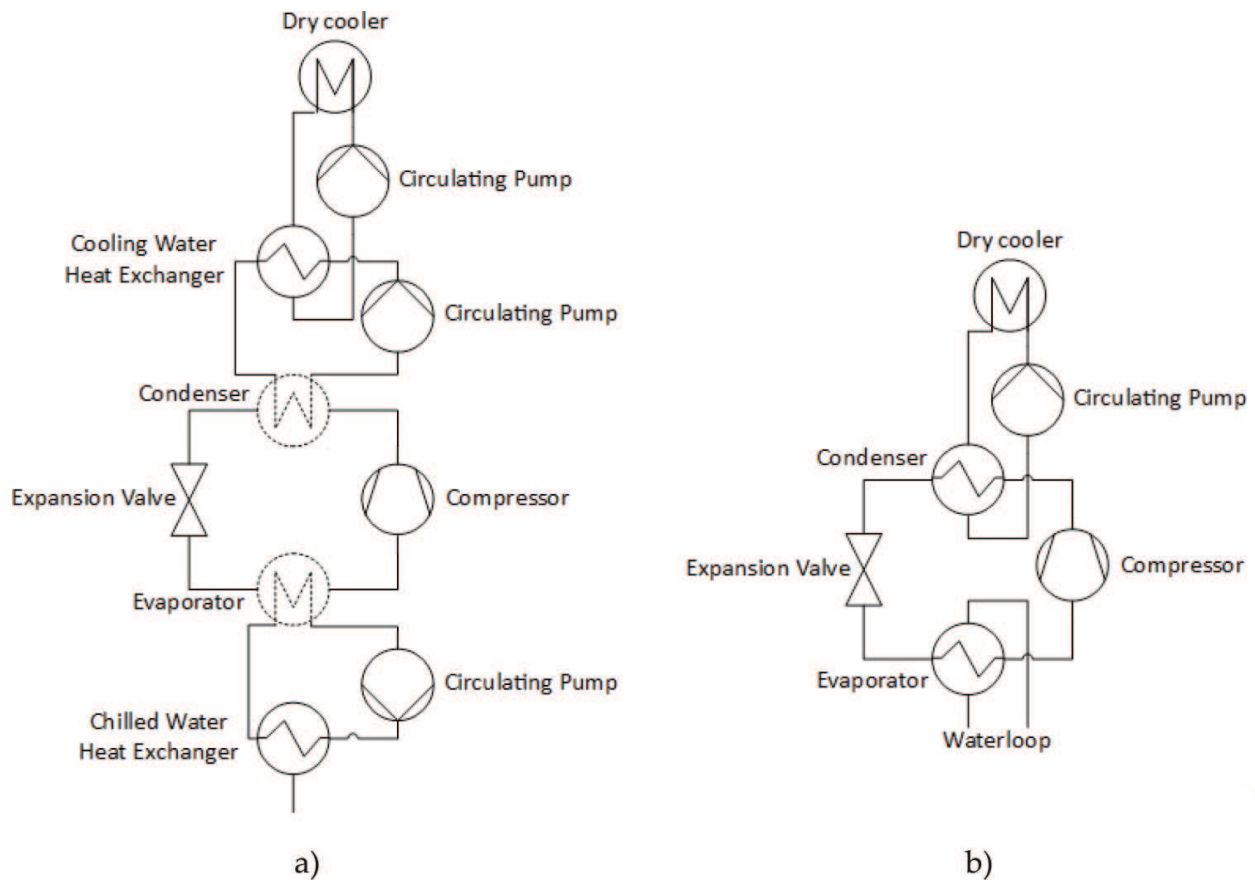**Figure 5.** Schematic of R744 refrigeration system.

Figure 6. (a) Schematic of a R718 refrigeration system with external heat exchangers (without i.c.). (b) Schematic of a R718 refrigeration system with integrated heat exchangers (with i.c.).

System (a) is a two-stage design with two identical refrigeration modules, with the first-stage condenser connected to the second-stage evaporator by a water interface. The required water circulation is generated by a circulating pump. Both condenser and evaporator are designed as open systems and, hence, the adapted, dashed symbol in the flow diagram. The heat transfer on the heat source as well as the heat sink side of the refrigeration system is done by braze plate heat exchangers. Again, a separate circulation pump is used for each circuit. Thus, a total of three pumps are required to operate the system in its present design stage.

System (b) differs from system (a) in the following points. The intermediate circle is not realized in this structure by a water interface but by a vapor interface with intermediate cooling (i.c.). Furthermore, the heat exchangers are integrated in the evaporator and condenser. Therefore, the three required internal circulation pumps in the system are obsolete.

4.1.3. Possible designs and combination of cascaded refrigeration processes

Table 2 lists the three system combinations under consideration. System 1 is a coupled system of a self-contained unit with a CO_2 compression refrigeration system, a water-loop and a dry cooler outside the building. The condenser/gas cooler of the CO_2 system is designed as a braze plate heat exchanger and represents the interface to the water-loop. The condensing heat is transported by means of the water-loop to the dry cooler, and this dissipates

System 1	CO_2 + water loop
System 2	CO_2 + water loop + R718 chiller without i.c. + external heat exchangers
System 3	CO_2 + water loop + R718 chiller with i.c. + integrated heat exchangers

Table 2. The different systems.

the waste heat to be ambient. In this system, the CO_2 process is subcritical or transcritical depending on the ambient temperature. As a result, all components must be designed for transcritical operation and the compressor for maximum load. These are then oversized for most of the year.

Systems 2 and 3 each consist of a self-contained unit with a CO_2 compression refrigeration system, a water-loop and an additional centrifugal compressor cooling system with water as refrigerant. This ensures that the CO_2 process can always be subcritical, as the water-loop always generates a constant water temperature for condensing CO_2 which is below the critical temperature of CO_2. The differences between Systems 2 and 3 are in the type of the R718 system used. System 2 is shown in **Figure 6(a)** and System 3 in **Figure 6(b)**.

The reference for the comparison is System 1.

4.2. Methods

For the qualitative assessment, the three systems were calculated with the following assumptions (**Table 3**). The physical properties for the cycle process calculation of the R718 process were generated using REFPROP [4].

R744		
Superheating	10	K
Cooling capacity (all systems)	22	kW
Evaporation temperature T_0	−5/−15	°C
$T_{GC/C}-T_{amb}$	4	K
R718		
Chilled water temperature	13.5/24.5	°C
Compressor efficiency	0.6	—
Electrical efficiency	0.8	—
$T_{c.w.}-T_{amb}$	4	K
Combination		
Maximum ambient temperature	35	°C
$T_{GC/C}-T_{WL}$	1.5	K

Table 3. Operating conditions.

The electrical power consumption of the R744 compressor was determined for all three systems by means of the manufacturer's design software [15] for the respective operating points. For all systems a constant power consumption of 400 W was assumed for each water-loop circulation pump. System 2 also took into account the electrical power consumption of the three internal circulation pumps with a constant power consumption of 500 W and the electrical power consumption of the two R718 centrifugal compressors. With System 3, the three pumps are eliminated, and thus only the two centrifugal compressors have been considered.

The electrical power consumption of the fans on the dry cooler or condenser/gas cooler has not been taken into account for the qualitative comparison of calculations in any system.

The exact calculations of the individual systems can be found in Formulas 1–3.

$$COP_1 = \frac{Q_0}{P_{R744} + P_{WL}} \tag{1}$$

$$COP_2 = \frac{Q_0}{P_{R744} + P_{WL} + P_{Pumps} + P_{R718}} \tag{2}$$

$$COP_3 = \frac{Q_0}{P_{R744} + P_{WL} + P_{R718}} \tag{3}$$

4.3. Results and comparison of the systems

As described in Section 2.4, System 1 is designed according to the maximum ambient temperature. Systems 2 and 3 are calculated with two condensing temperatures, 15 and 26°C. The required piston displacements of the carbon dioxide compressors for the indicated cooling capacity of 22 kW at −5 and −15°C evaporation temperature can be taken from **Table 4** for all three systems. The compressors were designed with frequency-controlled motors.

The required piston displacements are lower by a factor of two for Systems 2 and 3 than for System 1.

Figures 7 and **8** show the COP characteristics of the three systems above the ambient temperature. System 1 is used as the reference for the comparison of the systems, as described in Section 2.4. From both figures, it gets obvious that the switching point for the optimum energetic mode of operation depends on two factors:

- The evaporation temperature of the CO_2 process

- The condensation temperature of the CO_2 process

Systems	1	2/3	
	$T_C = 40.5°C$	$T_c = 26°C$	$T_c = 15°C$
$T_0 = -5°C$	9.6 m³ h⁻¹	6.5 m³ h⁻¹	4.8 m³ h⁻¹
$T_0 = -15°C$	12 m³ h⁻¹	9.6 m³ h⁻¹	6.5 m³ h⁻¹

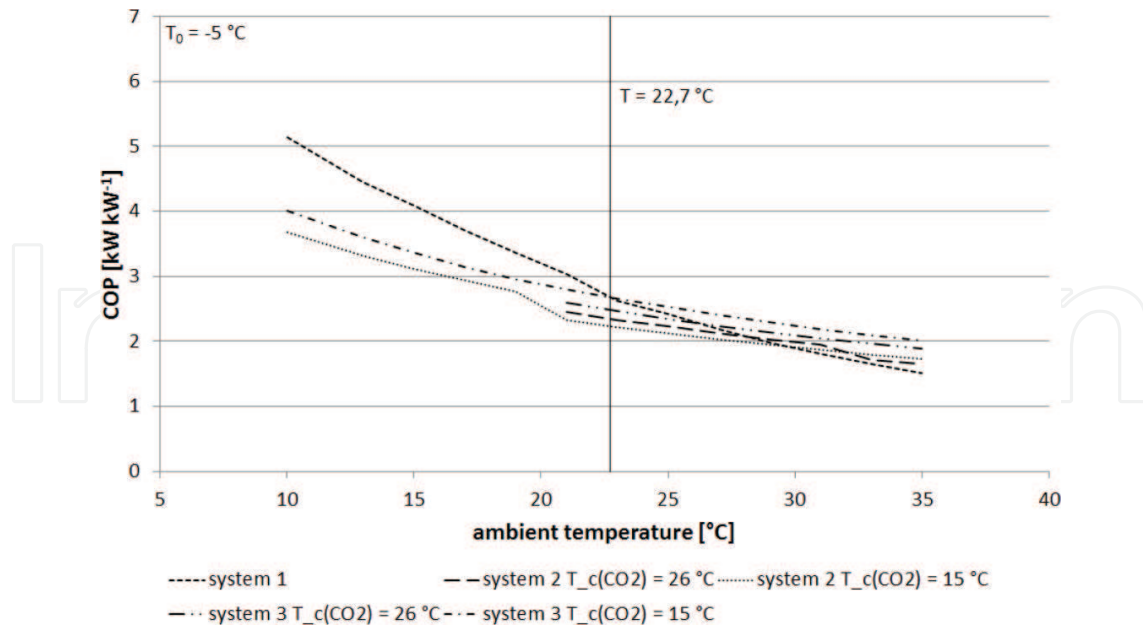**Table 4.** The required piston displacements of the carbon dioxide compressors depending on the system.
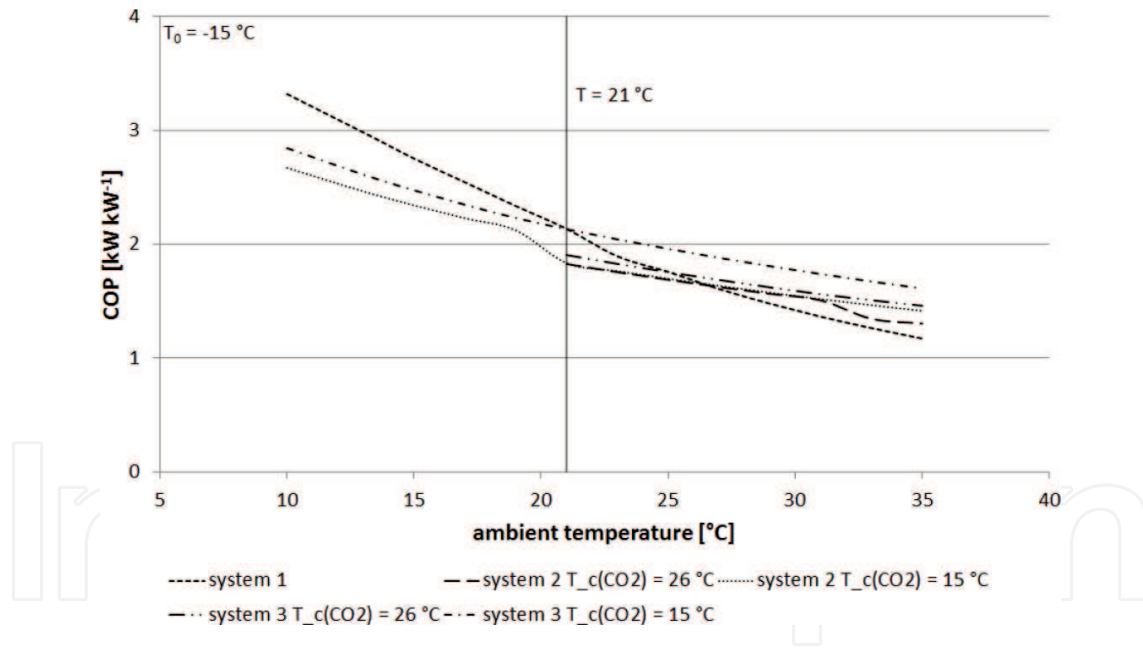
Figure 7. Comparison of the COP values at $T_0 = -5°C$.

Figure 8. Comparison of the COP values at $T_0 = -15°C$.

For both factors the statement applies, the lower, the better.

Thus, the switching point for $T_0 = -5°C$ and $T_C = 15°C$ at $T_{amb} = 22.7°C$ and for $T_0 = -15°C$ and $T_C = 15°C$ at $T_{amb} = 21°C$ compared with System 1. In both cases, System 3 has a significantly better energetic performance than System 2. This can be explained by the fact that in System 3 the circulating pumps of the R718 process can be dispensed with, and the losses in the water cycle between the two refrigeration modules are eliminated by using the intermediate cooling.

5. Mechanical subcooling of transcritical carbon dioxide

5.1. The investigated system

Figure 9 shows the schematic structure of the investigated system. It is a single-stage CO_2 cycle, the "refrigeration cycle," and a subcooling circuit "mechanical subcooling" downstream of the gas cooler. The aim is to further cool the transcritical CO_2 leaving the gas cooler by means of an additional compression refrigeration system. The refrigerant in this subcooling circuit is R718. The interface between the two circuits is a finned tube heat exchanger, which is traversed by CO_2 inside and is surrounded by circulating water in a vacuum atmosphere. The energy required for the evaporation of the water is taken from the CO_2 gas, thereby cooling it. The resulting water vapor is compressed by means of a centrifugal compressor and fed into the condenser. There, the water vapor rejects its energy to another finned tube heat exchanger to an additional cooling circuit and condenses completely. The circuit is then closed by a self-regulating, pressure loss-free expansion device. The expansion device used in combination with the continuously variable centrifugal compressor allows a continuous adjustment of the delivered volume flow, and the ratio between the condensing pressure and suction pressure of the compressor starts as low as at a value of "1."

The additional cooling circuit in the considered system consists of the heat exchanger, a circulation pump, and a dry cooler. As a working medium, a glycol/water brine is usually used. This extra circuit is needed because there are no commercially available air condensers for
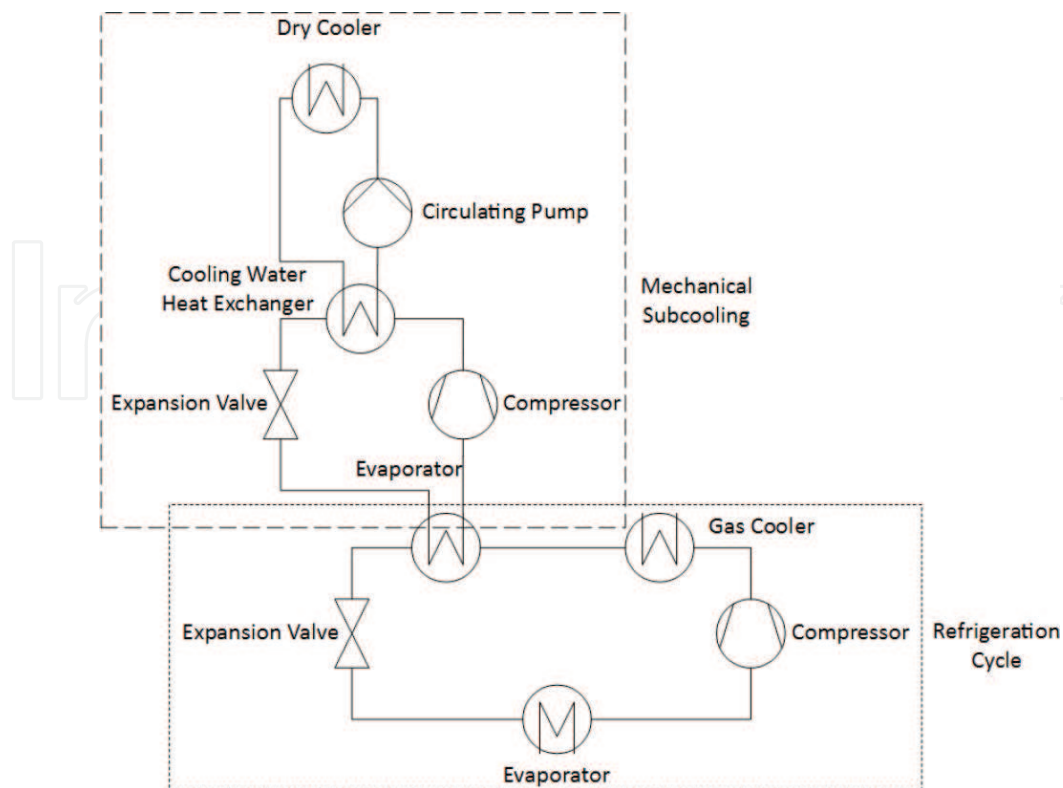

Figure 9. Schematic of the combined subcooling cycle.

R718. The problem is the given density ratio of >10,000, at a temperature of 50°C increasingly with decreasing water or steam temperature. Both systems, gas coolers and dry coolers, transfer their waste heat to the same heat sink, the environment.

5.2. Method

For the evaluation of the system with and without mechanical subcooling, the assumptions given in **Table 5** were used as the basis for the calculations. The physical properties of the refrigerants used for the respective cycles were generated with REFPROP [4].

For the calculation of the individual COP values, the electrical power consumption of the circulation pump in the external cooling water circuit of the R718 chiller as well as the fans of the gas cooler and the dry cooler were neglected. Only the specific capacities were considered. Eq. (4) shows the general calculation of COP, which is also used for the determination of pure transcritical operation. q_0 corresponds to the specific cooling capacity and w_c to the required specific compressor work of the refrigeration cycle.

$$COP = \frac{q_0}{w_c} \tag{4}$$

Eq. (5) shows the calculation of the specific cooling capacity and Eq. (6) the specific subcooling capacity of the CO_2 cycle. Eq. (7) shows the specific cooling capacity of the R718 circuit. h_0 and h_5 correspond to the specific enthalpy at the outlet of the evaporator or after the throttle, h_3 and h_4 to the specific enthalpy at the outlet of the gas cooler or after subcooling in the CO_2 cycle, and h_{1*} and h_{4*} to the specific enthalpy in the evaporator or after relaxing in the R718 circle.

$$q_{0,R744} = h_0 - h_5 \tag{5}$$

$$q_{sub} = h_3 - h_4 \tag{6}$$

$$q_{0,R718} = h_{1*} - h_{4*} \tag{7}$$

The energy balance of the subcooler is shown in Eq. (8), and Eq. (9) shows the relation of the occurring mass flows.

$$\dot{m}_{R744} * q_{sub} = \dot{m}_{R718} * q_{0,R718} \tag{8}$$

$$\dot{m}_{R718} = \frac{\dot{m}_{R744} * q_{sub}}{q_{0,R718}} \tag{9}$$

The specific compressor work of the two single-stage systems is shown in Eq. (10) for the R744 cycle and in Eq. (11) for the R718 process. h_1 and h_{1*} represent the specific enthalpy at the compressor inlet, h_2 and h_{2*} the isentropic specific enthalpy at the compressor outlet. $\eta_{i,R744}$ and $\eta_{i,R718}$ are the isentropic efficiencies of the respective compressors.

R744		
Superheating	10	K
Cooling capacity	150	kW
Evaporating temperature	−5/−15	°C
t_3-t_{env}	5	K
Isentropic compressor efficiency [16]	0.95–0.1*π	—
R718		
t_4-t_{1*}	5	K
compressor efficiency	0.7	—
t_{3*}-t_{env}	4	K
maximum compressor volume flow	1.2	m³ s⁻¹

Table 5. Operating conditions.

$$w_{c,R744} = \frac{h_{2,s} - h_1}{\eta_{i,R744}} \tag{10}$$

$$w_{c,R718} = \frac{h_{2*,s} - h_{1*}}{\eta_{i,R718}} \tag{11}$$

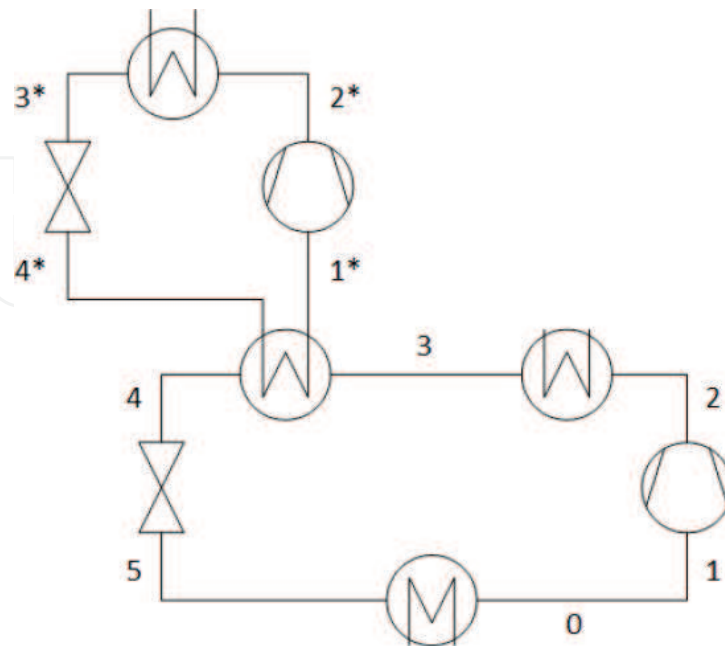Based on Eq. (4), the COP of the entire system is calculated in subcooling mode according to Eq. (12).

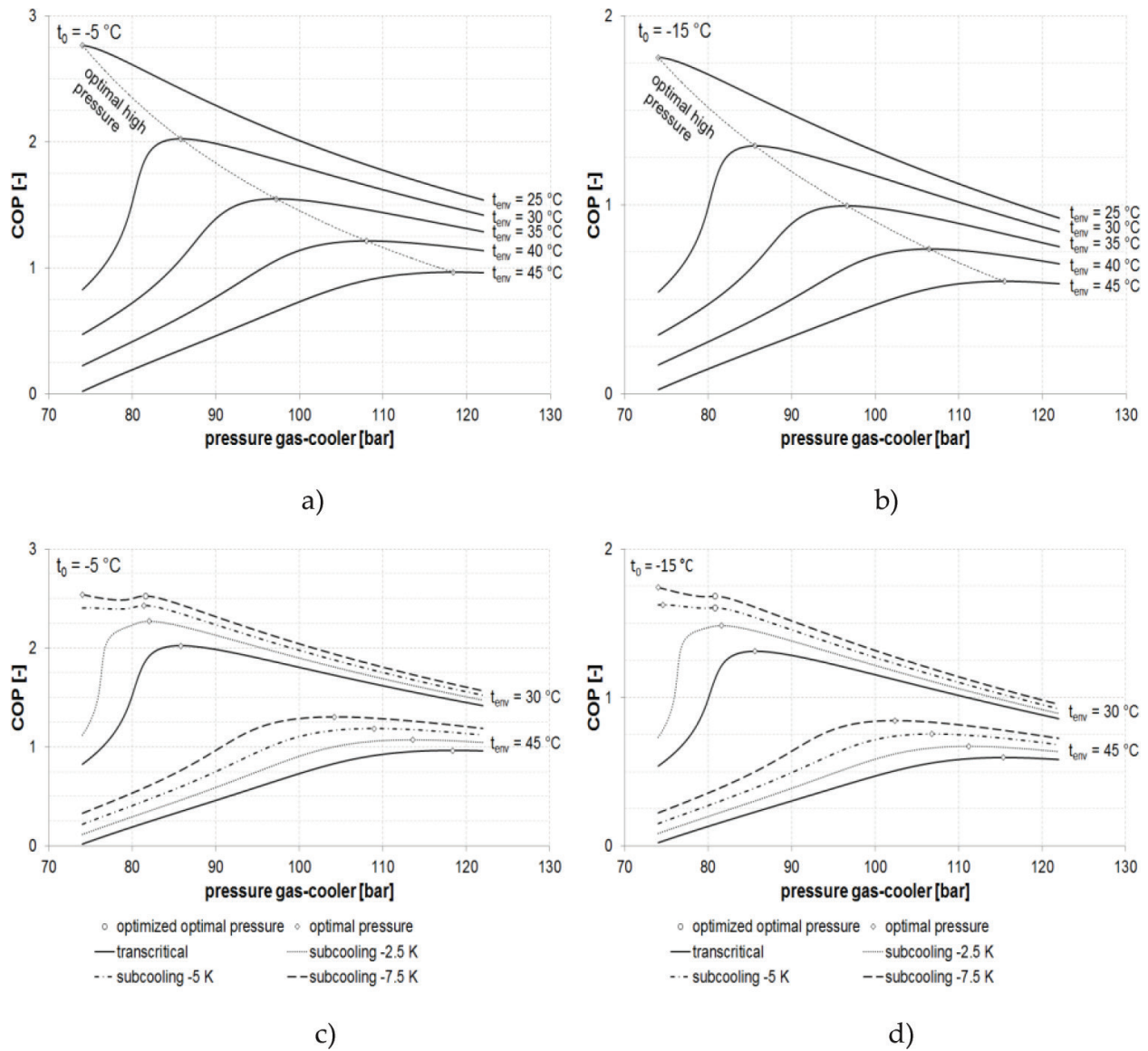**Figure 10.** Schematic with state points.

a)   b)

c)   d)

Figure 11. Optimal high pressure for the transcritical CO$_2$ cycle with (a) $t_0 = -5°C$ and (b) $t_0 = -15°C$; optimal and optimized pressure with subcooling for (c) $t_0 = -5°C$ and (d) $t_0 = -15°C$.

$$COP^* = \frac{\dot{m}_{R744} * q_{0,R744}}{\dot{m}_{R744} * w_{c,R744} + \dot{m}_{R718} * w_{c,R718}} = \frac{q_{0,R744}}{w_{c,R744} + \dfrac{q_{sub}}{q_{0,R718}} * w_{c,R718}} \qquad (12)$$

The individual states of the respective circuits are shown in **Figure 10**.

5.3. Results

5.3.1. Optimum operating conditions

Figure 11 shows the optimal high pressures of the transcritical CO$_2$ system, (a) for $t_0 = -5°C$ and (b) for $t_0 = -15°C$, for different ambient temperatures. The respective dashed lines represent the interpolated connections between the individual maximum points. The individual marked values have

been determined by means of a self-developed simulation. From each of the two diagrams, two curves at the ambient temperatures t_{env} = 30°C and t_{env} = 45°C are considered in more detail, and the optimal pressures for operation with a subcooling of −2.5, −5, and −7.5 K are shown. Diagram (c) shows the values for t_0 = −5°C, and diagram (d) shows the values t_0 = −15°C. In both diagrams, it can be seen that the optimum pressure drops as expected with increasing subcooling value. For (c) and (d), the optimum pressures at t_{env} = 30°C and a subcooling of 7.5 K at 74 bar and at (d) are only slightly higher when cooled by 5 K. This is followed by an increase in efficiency with subsequent increase in pressure, followed by a rise to a turning point. From this, the efficiency of the system continues to fall with further increases in process pressure. These inflection points are referred to in the diagrams as *optimized optimal pressure* and are preferable to the maximum efficiency points, since the efficiency values are only slightly lower and there are advantages for selecting the compressor for the subcooling stage. This can be explained by the p-h diagram shown in **Figure 12**.

The three illustrated cycles each show the transcritical CO_2 cycle for the operating point t_0 = −5°C and t_3 = 35°C. The solid line with the triangle symbols at the respective state points represents the pure transcritical cycle without mechanical subcooling at optimum high pressure. The dotted line with the circle symbols represents the transcritical cycle with a subcooling of 7.5 K at optimum high pressure (74 bars), and the dashed line with the rhombuses represents the transcritical cycle with subcooling at the optimized optimum pressure. The points 3 and 4 for the compared subcooling cycles are each on the same isotherms and represent at 3 the temperature at the gas cooler outlet and at 4 the temperature after the subcooling. Provided that the same cooling capacity is required for both systems, both systems need approximately the same mass flow of CO_2. If one compares the enthalpy difference q_{sub} with optimal and optimized optimal pressure, it clearly shows that the required subcooling performance at optimum pressure is more than a factor of two higher than that of the optimally optimized pressure. This would also result in a larger sizing of the R718 chiller.
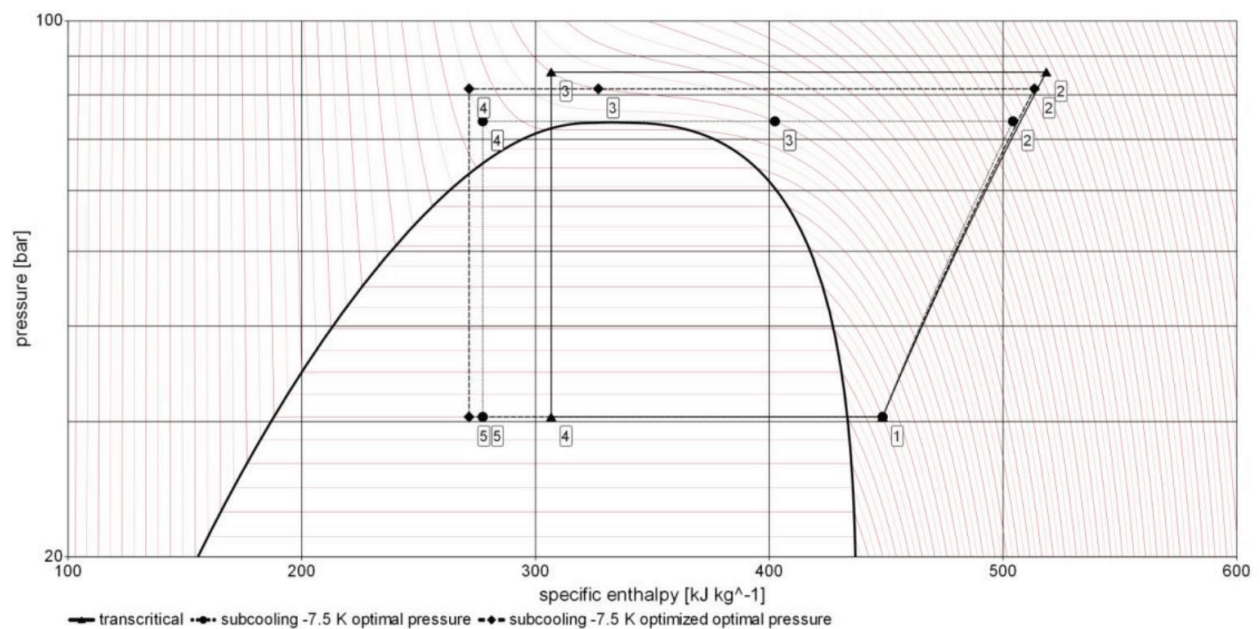

Figure 12. p-h diagram of the transcritical CO_2 cycle with and without mechanical subcooling (t_0 = −5°C, t_3 = 35°C).

5.3.2. Efficiency increase

Based on the optimum or optimized optimum operating pressures, **Figure 13** shows the COP curves for pure transcritical operation and for transcritical operation with mechanical sub-cooling as a function of the environment temperature. Diagram (a) refers to $t_0 = -5°C$ and diagram (b) to $t_0 = -15°C$. Furthermore, with the respective secondary axis, the efficiency increase between the purely transcritical operation and the operation with a subcooling of 7.5 K is shown. When comparing the two curves, it is noticeable that there is a dependency on the evaporation temperature and the ambient temperature. With decreasing evaporation temperature, as well as with increasing ambient temperature, the percentage increase in efficiency increases. Furthermore, it can be seen that the increase from an ambient temperature of $t_{env} = 35°C$ is significantly lower and seems to approach asymptotically to a maximum limit.

5.3.3. Required subcooling capacity

In the following, the required subcooling capacities (SUB) are shown in **Figure 14** with the solid lines, and the maximum possible cooling capacity (Q_0) of the R718 circuit for the three indicated subcooling temperatures is shown by the dashed lines. Diagram (a) refers to $t_0 = -5°C$ and diagram (b) to $t_0 = -15°C$. The optimized optimum pressure was used as the basis for the calculation.

It is easy to see that for both evaporating temperatures, with a small exception at $t_0 = -15°C$, with the single-stage R718 system, with the maximum volumetric flow given in **Table 5**, a subcooling of −5 K over the entire temperature range of the environment can be realized. Over a wide range, a subcooling value of >7.5 K is possible with the above setting. Again, for a subcooling of 7.5 K, as in **Figure 13**, a turning point in the curve at $t_{env} = 35°C$ can be seen. In addition, significantly larger subcooling temperatures are possible. Another point is the
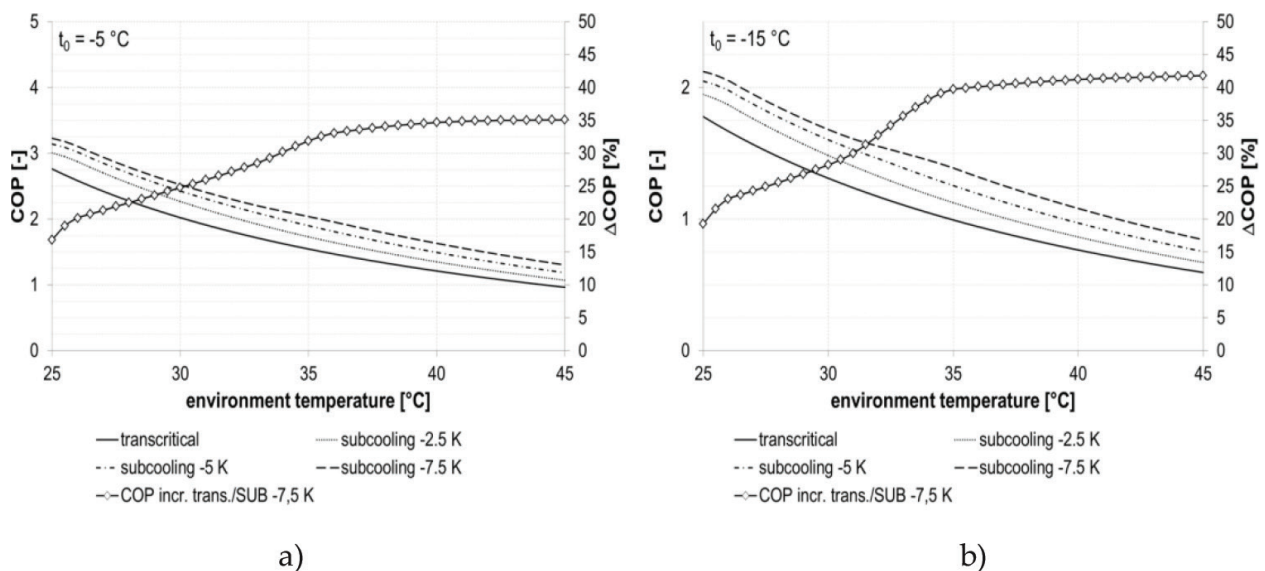

a)   b)

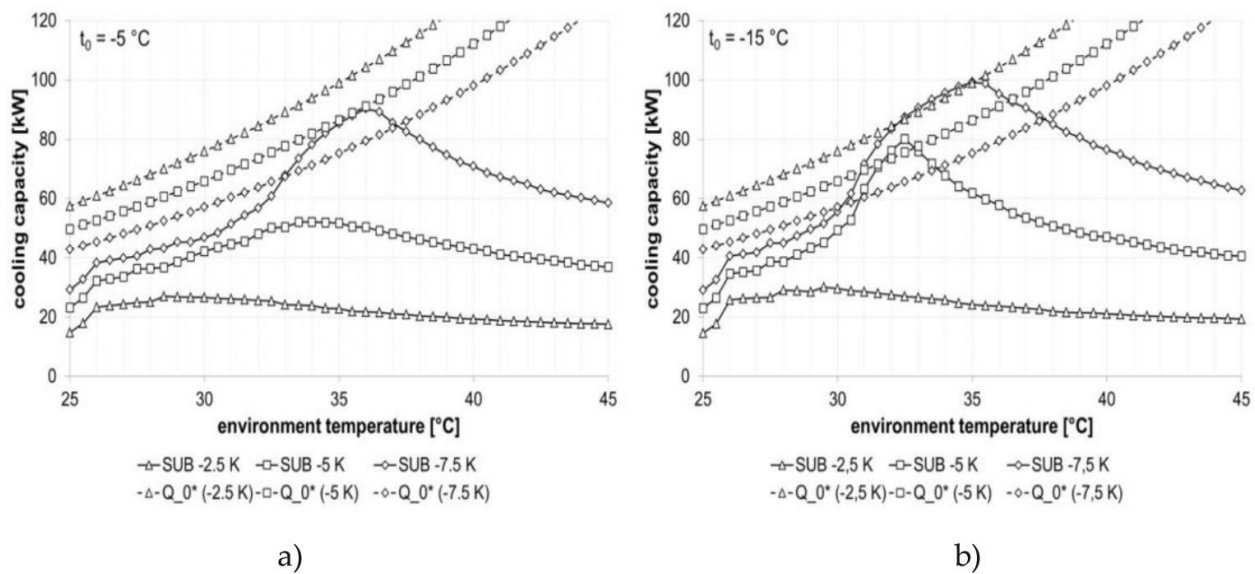**Figure 13.** COP of the transcritical CO_2 cycle with and without subcooling: (a) $t_0 = -5°C$ and (b) $t_0 = -15°C$.

Figure 14. Required subcooling capacity and possible cooling capacity: (a) $t_0 = -5°C$ and (b) $t_0 = -15°C$.

increasing possible cooling capacity with higher environment temperatures. This is related to the increase in the density of water vapor as the evaporation temperature increases.

In order to be able to subcool at least 7.5 K over the whole range of the environmental temperatures, there are two options for optimization. The first one could use a R718 compressor with a larger maximum flow rate, and, the second one could increase the process pressure at the outlet of the R744 compressor in order to reduce the required subcooling performance. Both options require further investigation to determine which of the two is more efficient. Furthermore, the combination of the two systems can still be examined to see what absolute subcooling over the entire environment temperature range for the two evaporation temperatures can be achieved.

6. Conclusion

The analysis of the systems has shown that a self-contained unit with water-loop combined with a centrifugal compressor cooling system with water as refrigerant of System 3 at a condensing temperature of $T_C = 15°C$ and an evaporation temperature of $T_0 = -15°C$ of the CO_2 process above an ambient temperature of $T_{amb} = 21°C$ proves to make sense from an energetic point of view. In addition to the energetic consideration, the positive effect of the subcritical design in contrast to System 1 has been noticed. It allows a much simpler design of the CO_2 system and the up to a factor 2 lower required piston displacements of the R744 compressors used.

The simulation of a transcritical CO_2 process with subsequent mechanical subcooling with a refrigeration system with the refrigerant R718 has shown that efficiency increases of more than 35% compared to purely transcritical operation can occur. The main influencing factors regarding the efficiency are on the one hand the evaporation and ambient temperatures and, on the other hand, the process pressure on the pressure side of the compressor. It has been

noticed that in the course of the COP curve above the environmental temperature, there are, in addition to the optimal process pressure, also points which have a positive effect on the entire system with a slight loss of efficiency. For both investigated evaporation temperatures in the CO_2 cycle, a subcooling of 5 K is possible with the considered system with a small exception over the entire ambient temperature range. Over much of the environmental temperatures, significantly greater temperature differences are possible. In order to allow a subcooling of 7.5 K over the entire temperature range, further investigations have to be made, which on the one hand consider a larger compressor and on the other hand a further optimized process pressure.

Nomenclature

COP	coefficient of performance (kW kW^{-1})
COP*	overall coefficient of performance (−)
GWP	global warming potential (−)
h	specific enthalpy (kJ kg^{-1})
$\dot{m}$	mass flow (kg s^{-1})
ODP	ozone depletion potential (−)
P	electrical power consumption (kW)
q_0	specific cooling capacity (kJ kg^{-1})
Q_0	cooling capacity (kW)
q_{sub}	specific subcooling capacity (kJ kg^{-1})
t_0	evaporating temperature (°C)
w_c	specific compression work (kJ kg^{-1})

Greek symbols

η	compressor efficiency (−)
π	pressure ratio (−)

Subscript

0…5	condition point of the CO_2 cycle
1*…4*	condition point of the R718 cycle
env	environment
Pumps	related to circulating pumps

R718   related to the R718 cycle

R744   related to the R744 cycle

WL   related to the water-loop circulating pump

Author details

Florian Hanslik* and Juergen Suess

*Address all correspondence to: florian.hanslik@efficient.energy.de

Efficient Energy GmbH, Feldkirchen, Germany

References

[1] European Commission. Regulation (EU) No 517/2014 of the European Parliament and of the Council of 16 April 2014 on fluorinated greenhouse gases and repealing Regulation (EC) No 842/2006: (OJ L 150 of 20.5.2014, pp. 195-230); 2014

[2] Kilicarslan A, Müller N. A comparative study of water as a refrigerant with some current refrigerants. International Journal of Energy Research. 2005;**29**:947-959. DOI: 10.1002/er.1084

[3] Suess J. A centrifugal compressor cooling system using water as working fluid. In: 12th IIR-Gustav Lorentzen Natural Working Fluids Conference (GL 2016); 21-24 August; Edinburgh, United Kingdom; 2016. pp. 1178-1184. DOI: 10.18462/iir.gl.2016.1204

[4] Lemmon EW, Huber ML, McLinden MO. NIST Reference Fluid Thermodynamic and Transport Properties Database (REFPROP); 2013

[5] Sasakura T. Report 2014 Sasakura Engineering Co., Ltd. 7-32 Takejima 4-chome, Nishi-yodogawa-ku, Osaka 555-0011, Japan

[6] Ophir A. Mechanical heat pumps using water as refrigerant for ice production and air conditioning. In: IDEA 99th Annual Converence & Trade Show, Orlando, Florida; 2008

[7] Albring P. Kältetechnik mit Wasser als Kältemittel, Netzwerk Kältetechnik; 2009

[8] Albring P, Honke M. Ice-making and ice storage, with water as refrigerant. In: 23rd IIR International Congress of Refrigeration; 21-26 August; Prague, Czech Republic; 2011

[9] Li Q, Piechna J, Müller N. Thermodynamic potential of using a counter rotating novel axial impeller to compress water vapor as refrigerant. International Journal of Refrigeration. 2011;**34**:1286-1295. DOI: 10.1016/j.ijrefrig.2011.03.002

[10] Borup J, Jensen J. Udvikling af Rotrex turbokompressor til vanddamp compression, Nr. 344-009, PSO Program 2012, Dansk Energi

[11] Murayama S. Report 2014 Kawasaki Heavy Industries, Ltd. Tokyo Office, 14-5 Kaigan 1-chrome, Minato-ku, Tokyo 105-8315, Japan

[12] Honke M, Safarik M, Herzog R. R718 turbo chillers and vacuum ice generation–Two applications of a new generation of high speed, high capacity R718 centrifugal compressors. In: 24th IIR International Congress of Refrigeration; 16-22 August; Yokohama, Japan; 2015

[13] Madsbøll H. Competitive Chiller Concept with Water as Refrigerant, Danske Køledage; 2013

[14] Süß J. Eine kompakte Kälteanlage mit Wasser als Kältemittel. In: Deutsche Kälte- und Klimatagung; 19-21 November 2014; Düsseldorf; 2014

[15] Bitzer. BITZER Software, Version 6.7.0.1849. 2017. https://www.bitzer.de/de/de/software/ [Accessed: November 2, 2017]

[16] Llopis R, Cabello R, Sánchez D, Torrella E. Energy improvements of CO_2 transcritical refrigeration cycles using dedicated mechanical subcooling. International Journal of Refrigeration. 2015;**55**:129-141. DOI: 10.1016/j.ijrefrig.2015.03.016